Fluid model of electron cyclotron current drive

G. O. Ludwig

Associated Plasma Laboratory, National Space Research Institute
12227-010 São José dos Campos, SP, Brazil

Abstract. A macroscopic model is proposed to describe the dynamics of electron cyclotron current drive (ECCD). This model depends on the adoption of a suitable distribution function for the energetic current-carrying electrons. The model is readily applied to examine the current drive efficiency of high-power ECCD experiments, reproducing the main experimental features.

Keywords: ECR, Current drive
PACS: 52.50.Sw, 52.55.Wq

INTRODUCTION

Localized current drive by electron cyclotron waves is a powerful technique that has received extensive experimental treatment [1, 2, 3, 4]. Overall, the experimental results are in good agreement with simulations using three-dimensional quasi-linear Fokker-Planck codes [3]. However, these cumbersome codes are not convenient for modeling comprehensive tokamak systems or time dependent scenarios. As an alternate, this paper describes a macroscopic model of ECCD. It is based on a previous work [5], improving the form of the distribution function for the magnetized relativistic electron stream. Simplified expressions of power and force densities are derived from quasi-linear diffusion. The results of the model are compared to experimental measurements of current drive on the DIII-D and TCV tokamaks.

MOMENTS OF THE FOKKER-PLANCK EQUATION

Neglecting radial transport effects the Fokker-Planck equation for streaming electrons is

$$\frac{\partial f}{\partial t} = -\nabla_p \cdot \left(\vec{\Gamma}_c + \vec{\Gamma}_E + \vec{\Gamma}_{RF} \right) = -\nabla_p \cdot \vec{\Gamma}, \tag{1}$$

where $\vec{\Gamma}_c$ is the collisional flux, and the driving fluxes due to both a slow varying inductive electric field and diffusion by RF waves are given, respectively, by

$$\begin{aligned} \vec{\Gamma}_E &= -eE_\parallel f \widehat{e}_\parallel, \\ \vec{\Gamma}_{RF} &= -\overline{\overline{D}}_{RF} \cdot \nabla_p f, \end{aligned} \tag{2}$$

where e is the electron charge, $\widehat{e}_\parallel$ is the unit vector in the direction of the magnetic field, and $\overline{\overline{D}}_{RF}$ is the quasi-linear RF diffusion dyadic.

A general moment is obtained multiplying the Fokker-Planck equation by a momentum-dependent quantity $\Phi(\overrightarrow{p})$ and integrating over all momentum space

$$\frac{\partial}{\partial t}(n\langle\Phi\rangle) = \int \overrightarrow{\Gamma} \cdot \nabla_p \Phi(\overrightarrow{p})\, d^3p. \tag{3}$$

The rates of change of the kinetic energy $\Phi = m_e c^2(\gamma - 1)$ and momentum $\overrightarrow{\Phi} = \overrightarrow{p} = m_e c \gamma \overrightarrow{\beta}$, where $\gamma = \sqrt{1 + p^2/(m_e^2 c^2)} = 1/\sqrt{1-\beta^2}$, give the equations of motion

$$\begin{aligned} \tfrac{\partial}{\partial t}\langle\gamma - 1\rangle &= -\nu_c \left\langle \tfrac{\gamma}{\left(\gamma^2-1\right)^{1/2}} \right\rangle + \tfrac{P_d}{n m_e c^2}, \\ \tfrac{\partial}{\partial t}\left\langle \gamma\overrightarrow{\beta} \right\rangle &= -\nu_c \left\langle \tfrac{(1+Z+\gamma)\gamma^2}{\left(\gamma^2-1\right)^{3/2}} \overrightarrow{\beta} \right\rangle + \tfrac{\overrightarrow{F}_d}{n m_e c}, \end{aligned} \tag{4}$$

where ν_c is the collision frequency (normalized to the speed of light) of energetic electrons colliding with a thermal background of electrons and ions of charge Z

$$\nu_c = \frac{n_e e^4 \ln\Lambda_{e'e}}{4\pi\varepsilon_0^2 m_e^2 c^3}, \tag{5}$$

and where e' and e designate the energetic and plasma electrons, respectively. The volumetric densities of driven power, P_d, and force, $\overrightarrow{F}_d$, are given in terms of the driving fluxes by:

$$\begin{aligned} P_d &= -neE_\parallel c\left\langle \beta_\parallel \right\rangle - c\int\left(\overrightarrow{\beta} \cdot \overline{\overline{D}}_{RF} \cdot \nabla_p f\right) d^3p, \\ \overrightarrow{F}_d &= -neE_\parallel \widehat{e}_\parallel - \int\left(\overline{\overline{D}}_{RF} \cdot \nabla_p f\right) d^3p. \end{aligned} \tag{6}$$

These quantities must satisfy the electrodynamic constraint

$$P_d = c\overrightarrow{F}_d \cdot \left\langle \overrightarrow{\beta} \right\rangle, \tag{7}$$

which gives the rate at which the RF energy is being converted to kinetic energy per unit volume. The equations of motion (4) correspond, assuming a mono-energetic stream and neglecting the external sources, to the Langevin equations which describe the slowing down of energy and momentum of test electrons.

QUASI-LINEAR RF DIFFUSION DYADIC

In cylindrical coordinates in momentum space the gyro-averaged quasi-linear diffusion dyadic is

$$\overline{\overline{D}}_{RF} = D_\perp \widehat{e}_\perp \widehat{e}_\perp + D_\wedge\left(\widehat{e}_\perp \widehat{e}_\parallel + \widehat{e}_\parallel \widehat{e}_\perp\right) + D_\parallel \widehat{e}_\parallel \widehat{e}_\parallel. \tag{8}$$

Substituting in the expressions of the power and force per unit volume (6) yields

$$
\begin{aligned}
P_d &= -neE_{\|}c\left\langle\beta_{\|}\right\rangle - nc\left\langle\left(\beta_\perp D_\perp + \beta_{\|}D_\wedge\right)\frac{\partial}{\partial p_\perp}\ln f + \left(\beta_\perp D_\wedge + \beta_{\|}D_{\|}\right)\frac{\partial}{\partial p_{\|}}\ln f\right\rangle, \\
\overrightarrow{F}_d &= -neE_{\|}\widehat{e}_{\|} - n\left\langle D_\perp\frac{\partial}{\partial p_\perp}\ln f + D_\wedge\frac{\partial}{\partial p_{\|}}\ln f\right\rangle\widehat{e}_\perp - n\left\langle D_\wedge\frac{\partial}{\partial p_\perp}\ln f + D_{\|}\frac{\partial}{\partial p_{\|}}\ln f\right\rangle\widehat{e}_{\|} \\
&= F_\perp\widehat{e}_\perp + F_{\|}\widehat{e}_{\|}.
\end{aligned} \tag{9}
$$

In the small gyroradius limit $k_\perp v_\perp/(\Omega_e/\gamma) \ll 1$, with $\Omega_e = eB/m_e$, the diffusion coefficients for the fundamental resonance of electron cyclotron waves are given by

$$
\begin{aligned}
D_\perp &\cong \frac{D_0}{|\beta_{\|}|}\left(\frac{\Omega_e}{\gamma\omega}\right)^2\Delta(\xi), \\
D_\wedge &\cong \frac{D_0}{|\beta_{\|}|}\left(1-\frac{\Omega_e}{\gamma\omega}\right)\frac{\Omega_e}{\gamma\omega}\frac{\beta_\perp}{\beta_{\|}}\Delta(\xi), \\
D_{\|} &\cong \frac{D_0}{|\beta_{\|}|}\left(1-\frac{\Omega_e}{\gamma\omega}\right)^2\frac{\beta_\perp^2}{\beta_{\|}^2}\Delta(\xi),
\end{aligned} \tag{10}
$$

where $D_0 = \pi e^2\overline{E_\perp^2}/\omega$ is the diffusion coefficient strength expressed in terms of the effective perpendicular wave amplitude, and $\xi = [1-\Omega_e/(\gamma\omega)]/\beta_{\|}$ is the refractive index variable along the wave spectrum. For a narrow spectrum centered at the refracting index $n_{\|}$, within a small range $\Delta n_{\|}$, the dimensionless function $\Delta(\xi)$ has the characteristics of a delta-function with unit area and amplitude proportional to $1/\Delta n_{\|}$ at $\xi = n_{\|}$, i.e. $\Delta(\xi) \sim \delta\left(\xi - n_{\|}\right)$.

Performing the transformation $\left(\xi,\beta_{\|}\right) \rightarrow \left(\pi p_\perp^2, p_{\|}\right)$ defined by

$$
\begin{aligned}
\pi p_\perp^2 &= \pi m_e^2c^2\left[\left(\frac{\Omega_e}{\omega}\right)^2\frac{1-\beta_{\|}^2}{\left(1-\beta_{\|}\xi\right)^2} - 1\right], \\
p_{\|} &= m_ec\frac{\Omega_e}{\omega}\frac{\beta_{\|}}{1-\beta_{\|}\xi}, \\
|J| &= 2\pi m_e^3c^3\left(\frac{\Omega_e}{\omega}\right)^3\frac{|\beta_{\|}|}{\left(1-\beta_{\|}\xi\right)^4},
\end{aligned} \tag{11}
$$

where $|J|$ is the Jacobian determinant, the moments of the Fokker-Planck equation are expressed in the variables $\left(\xi,\beta_{\|}\right)$ by

$$
\langle\Phi(\overrightarrow{p})\rangle = \frac{2\pi m_e^3c^3}{n}\left(\frac{\Omega_e}{\omega}\right)^3\int f\left(\xi,\beta_{\|}\right)\frac{\Phi\left(\xi,\beta_{\|}\right)\Delta(\xi)\left|\beta_{\|}\right|}{\left(1-\beta_{\|}\xi\right)^4}d\xi d\beta_{\|}. \tag{12}
$$

In the limit $\Delta n_{\|} \rightarrow 0$ the function $\Delta(\xi)$ becomes a delta function, giving the leading terms in the asymptotic expansions of integrals over the wave spectrum for $\left|n_{\|}\right| < 1$:

$$
\left\langle\Phi\left(\xi,\beta_{\|}\right)\right\rangle_{\xi=n_{\|}} \sim \frac{2\pi m_e^3c^3}{n}\left(\frac{\Omega_e}{\omega}\right)^3\int f\left(n_{\|},\beta_{\|}\right)\frac{\Phi\left(n_{\|},\beta_{\|}\right)\left|\beta_{\|}\right|}{\left(1-n_{\|}\beta_{\|}\right)^4}d\beta_{\|}. \tag{13}
$$

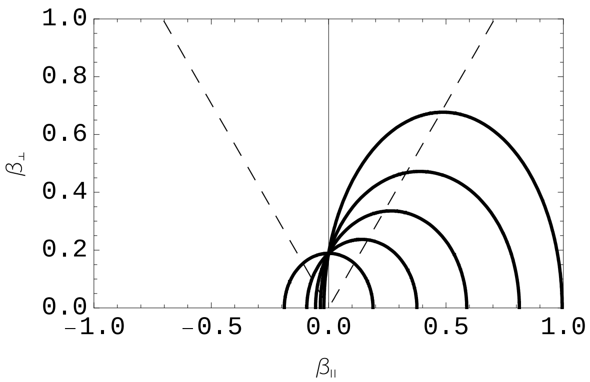

FIGURE 1. Resonance lines in velocity space normalized to the speed of light for $\omega = 0.982\Omega_e$. The curves correspond to values of the refractive index $n_\parallel = 0$, 0.15, 0.3, 0.5, 0.9 from center to edge. The dashed lines represent the trapped particle region for a mirror ratio 2/3, although the present model does not include its effect.

The leading terms in the expressions of the power and force densities are

$$\begin{aligned}
P_d &\sim -neE_\parallel c\left\langle\beta_\parallel\right\rangle - \tfrac{nD_0}{m_e}\left\langle \tfrac{\beta_\perp^2}{|\beta_\parallel|}\left(\tfrac{\Omega_e}{\omega}2m_e^2c^2\tfrac{\partial}{\partial p_\perp^2}\ln f + n_\parallel m_e c\tfrac{\partial}{\partial p_\parallel}\ln f\right)\right\rangle_{\xi=n_\parallel} \\
&= -neE_\parallel c\left\langle\beta_\parallel\right\rangle + P_{RF}, \\
F_\perp &\sim -\tfrac{nD_0}{m_e c}\left\langle \tfrac{\beta_\perp}{|\beta_\parallel|}\left(1-n_\parallel\beta_\parallel\right)\left(\tfrac{\Omega_e}{\omega}2m_e^2c^2\tfrac{\partial}{\partial p_\perp^2}\ln f + n_\parallel m_e c\tfrac{\partial}{\partial p_\parallel}\ln f\right)\right\rangle_{\xi=n_\parallel}, \\
F_\parallel &\sim -neE_\parallel + n_\parallel\tfrac{P_{RF}}{c},
\end{aligned} \tag{14}$$

where

$$\beta_\perp^2 = 1-\beta_\parallel^2 - \left(\frac{\omega}{\Omega_e}\right)^2\left(1-n_\parallel\beta_\parallel\right)^2 \tag{15}$$

corresponds to the resonance lines shown in Fig. (1). The integration limits in (14) are defined by the two roots of $\beta_\perp^2$:

$$\beta_\pm = \frac{n_\parallel \pm (\Omega_e/\omega)\sqrt{(\Omega_e/\omega)^2+n_\parallel^2-1}}{(\Omega_e/\omega)^2+n_\parallel^2}. \tag{16}$$

The expressions (14) give the macroscopic manifestations of interaction between the energetic particles and both the inductive electric field and a narrow spectrum of superluminous parallel phase velocity electron-cyclotron waves in the first harmonic EC regime.

DISTRIBUTION FUNCTION OF THE ELECTRON STREAM

A suitable form of the distribution function for the energetic electrons is necessary to evaluate moments of the Fokker-Planck equation, giving the macroscopic rates of change of momentum and energy. As shown in Ref. [6], the distribution function of a weakly collisional, strongly magnetized relativistic electron stream can be written as a sum of Dory-Guest-Harris components of the form

$$f_\ell = \frac{n_\ell \sqrt{1-\langle\beta_\parallel\rangle^2}}{4\pi m_e^3 c^3} C_\ell\left(\overset{0}{T},\overset{0}{T}_\parallel\right)\left(\frac{p_\perp^2}{2m_e\overset{0}{T}}\right)^\ell \exp\left(\frac{m_e c^2}{\overset{0}{T}_\parallel} - \frac{\gamma m_e c^2 - c\langle\beta_\parallel\rangle p_\parallel}{\overset{0}{T}_\parallel\sqrt{1-\langle\beta_\parallel\rangle^2}} - \frac{p_\perp^2}{2m_e\overset{0}{T}}\right), \tag{17}$$

where n_ℓ is the number density of the component ℓ, $c\langle\beta_\parallel\rangle$ is the average velocity of the streaming electrons in the direction of the magnetic field $\overrightarrow{B} = B\widehat{e}_\parallel$, and $\overset{0}{T}_\parallel$ is the parallel temperature expressed in energy units in the rest frame of the stream. The parameter $\overset{0}{T}$ determines the degree of magnetization and the index $\ell = 0,1,2\ldots$ gives a measure of the anisotropy in the perpendicular direction. The bi-Maxwellian distribution corresponds to $\ell = 0$. The density and temperature parameters satisfy the Lorentz transformation properties

$$\overset{0}{n}_\ell = n_\ell\sqrt{1-\langle\beta_\parallel\rangle^2} \quad , \quad \overset{0}{T}_\parallel = \frac{T_\parallel}{\sqrt{1-\langle\beta_\parallel\rangle^2}} \quad \text{and} \quad \overset{0}{T} = T, \tag{18}$$

so that the parallel pressure associated with the component ℓ,

$$\overset{0}{P}_{\parallel,\ell} = \overset{0}{n}_\ell\overset{0}{T}_\parallel, \tag{19}$$

follows the perfect gas law and becomes a Lorentz invariant. The normalization coefficient $C_\ell\left(\overset{0}{T},\overset{0}{T}_\parallel\right)$ is given as the inverse of a series in terms of modified Bessel functions of the second kind $K_\nu(z)$

$$C_\ell\left(\overset{0}{T},\overset{0}{T}_\parallel\right) = \left[\left(\frac{\overset{0}{T}_\parallel}{m_e c^2}\right)\exp\left(\frac{m_e c^2}{\overset{0}{T}_\parallel}\right)\left(\frac{\overset{0}{T}_\parallel}{\overset{0}{T}}\right)^\ell \sum_{k=0}^\infty \frac{(\ell+k)!}{k!}\left(-\frac{\overset{0}{T}_\parallel}{\overset{0}{T}}\right)^k K_{\ell+k+2}\left(\frac{m_e c^2}{\overset{0}{T}_\parallel}\right)\right]^{-1}. \tag{20}$$

This series is appropriate for calculations with $\overset{0}{T}_\parallel \ll \overset{0}{T}$. A power series expansion to second order in $\overset{0}{T}_\parallel/\left(m_e c^2\right)$ valid for $0 < \overset{0}{T} < \infty$ is given in [6]. Taking $\ell = 0$, $\overset{0}{T} \to \infty$ and $\langle\beta_\parallel\rangle = 0$ in (17) recovers the Jüttner distribution for an isotropic relativistic electron gas. Using the distribution function in the form (17), the thermodynamic quantities and equations of state pertaining to an anisotropic relativistic electron stream can be obtained. In particular, the Chew-Goldberger-Low double adiabatic equations are recovered in the warm plasma limit $\overset{0}{T}_\parallel \ll \left(m_e c^2\right)$.

The energy density, the magnetization, and the enthalpy density of the component ℓ are defined in the rest frame of the electron stream by, respectively,

$$
\begin{aligned}
\overset{0}{U}_{\ell} &= \overset{0}{n}_{\ell} m_e c^2 \langle \gamma \rangle , \\
\overset{0}{M}_{\ell} &= -\overset{0}{n}_{\ell} \left\langle \frac{p_\perp^2}{2 m_e B} \right\rangle , \\
\overset{0}{H}_{\ell} &= \overset{0}{U}_{\ell} + \overset{0}{P}_{\parallel,\ell} - B \overset{0}{M}_{\ell} - \ell \overset{0}{P}_{\parallel,\ell} \left\langle \ln \left(\frac{p_\perp^2}{2 m_e \overset{0}{T}} \right) \right\rangle .
\end{aligned}
\tag{21}
$$

These quantities can be calculated in the laboratory frame applying a boost with velocity $c \langle \beta_\parallel \rangle$. The Lorentz invariant perpendicular pressure of component ℓ is

$$
\overset{0}{P}_{\perp,\ell} = \left(1 + \ell + \frac{B \overset{0}{M}_{\ell}}{\overset{0}{n}_{\ell} \overset{0}{T}} \right) \overset{0}{P}_{\parallel,\ell} . \tag{22}
$$

Now, the electron stream distribution function in ECCD is written as a sum of components of type (17). In particular, as a sum of $\ell = 0$ (bi-Maxwellian) and $\ell = 1$ DGH-like components

$$
f = \sum_{\ell} f_{\ell} = f_0 + f_1 . \tag{23}
$$

This form of the distribution function corresponds to an excited state that can be taken only as a model. The actual distribution will depend, in general, on the detailed drive mechanism of high-energy electrons and the equilibration time. Also, depending on the degree of anisotropy this distribution is prone to the Weibel instability that possibly occurs in ECCD. Nevertheless, the main objective of this paper is to show that the proposed form of the distribution function gives consistent macroscopic results for ECCD.

The total parallel pressure follows Dalton's law with the same parallel temperature for each component

$$
\overset{0}{P}_{\parallel} = \sum_{\ell} \overset{0}{P}_{\parallel,\ell} = \overset{0}{n} \overset{0}{T}_{\parallel} , \tag{24}
$$

and the total perpendicular pressure depends on the degree of magnetization according with

$$
\overset{0}{P}_{\perp} = \sum_{\ell} \overset{0}{P}_{\perp,\ell} = \left(1 + F + \frac{B \overset{0}{M}}{\overset{0}{n} \overset{0}{T}} \right) \overset{0}{P}_{\parallel} = \overset{0}{n} \overset{0}{T}_{\perp} , \tag{25}
$$

which introduces the total magnetization $\overset{0}{M} = \sum_{\ell} \overset{0}{M}_{\ell}$ and defines the perpendicular temperature $\overset{0}{T}_{\perp}$, and where $F = \overset{0}{n}_1 / \overset{0}{n} = n_1 / n$ is a Lorentz invariant giving the ratio between the density of the $\ell = 1$ component and the total electron stream density. All components have the same degree of magnetization specified by the parameter $\overset{0}{T} = T$ (the components with $\ell > 0$ intrinsically correspond to states of higher magnetic susceptibility). It is also assumed that the average velocity $c \langle \beta_\parallel \rangle$ is the same for all components.

One verifies that for a strongly magnetized electron stream the perpendicular temperature vanishes, that is, $\overset{0}{T}_\perp \sim 0$ as $\overset{0}{T} \to 0$, and attains a maximum $\overset{0}{T}_\perp \sim (1+F)\overset{0}{T}_\parallel$ when $\overset{0}{T} \to \infty$, corresponding to the state of highest demagnetization. Indeed, for a warm electron stream, i.e. $\overset{0}{T}_\parallel \ll m_e c^2$, the perpendicular temperature is given approximately by

$$\overset{0}{T}_\perp \cong \frac{(1+F)\overset{0}{T}\overset{0}{T}_\parallel}{\overset{0}{T}+\overset{0}{T}_\parallel}, \tag{26}$$

and the magnetic susceptibility of the stream is

$$\overset{0}{\chi}_m = \frac{\mu_0 \overset{0}{M}}{B} \cong -\frac{(1+F)\overset{0}{T}}{\overset{0}{T}+\overset{0}{T}_\parallel}\frac{\overset{0}{P}_\parallel}{B^2/\mu_0}. \tag{27}$$

Also, in the warm stream limit, the energy density becomes

$$\overset{0}{U} = \sum_\ell \overset{0}{U}_\ell \cong \overset{0}{n} m_e c^2 + \frac{\overset{0}{P}_\parallel}{\gamma_p - 1}, \tag{28}$$

where γ_p is the "polytropic" index

$$\gamma_p = \frac{2\overset{0}{T}_\perp + 3\overset{0}{T}_\parallel}{2\overset{0}{T}_\perp + \overset{0}{T}_\parallel}. \tag{29}$$

The proposed form (23) of the distribution function of the streaming electrons is characterized by the average velocity $\langle \beta_\parallel \rangle$ plus the three parameters F, $\overset{0}{T}_\parallel$ and $\overset{0}{T}$ that enter the rest frame equations of state for $\overset{0}{U}$, $\overset{0}{M}$ and $\overset{0}{H}$. In general, the total enthalpy density in the rest frame of the electron stream can be written as

$$\overset{0}{H} = \sum_\ell \overset{0}{H}_\ell = \overset{0}{U} + \overset{0}{P}_\parallel + \left(\overset{0}{P}_\parallel - \overset{0}{P}_\perp\right) + F\overset{0}{P}_\parallel \left[1 - \left\langle \ln\left(\frac{p_\perp^2}{2m_e\overset{0}{T}}\right)\right\rangle\right] \tag{30}$$

which becomes, in the warm stream limit,

$$\overset{0}{H} \cong \overset{0}{n} m_e c^2 + \frac{5}{2}\overset{0}{P}_\parallel + F\overset{0}{P}_\parallel \left[\gamma_E + \ln\left(\frac{\overset{0}{T}+\overset{0}{T}_\parallel}{\overset{0}{T}_\parallel}\right)\right], \tag{31}$$

where $\gamma_E \cong 0.577$ is the Euler gamma.

MACROSCOPIC MODEL OF ECCD DISCHARGES

Using the electron stream distribution function specified by (17) and (23) one evaluates the macroscopic quantities needed in the equations of motion (4), namely, the average rates of energy and parallel momentum loss by collisions, given in normalized form respectively by

$$\left\langle \frac{\gamma}{\left(\gamma^2-1\right)^{1/2}} \right\rangle \quad \text{and} \quad \left\langle \frac{(1+Z+\gamma)\gamma^2}{\left(\gamma^2-1\right)^{3/2}} \beta_\| \right\rangle, \tag{32}$$

and the average perpendicular velocity $\langle \beta_\perp \rangle$, which satisfies the electrodynamic constraint (7)

$$\langle \beta_\perp \rangle \sim \frac{\left(1 - n_\| \left\langle \beta_\| \right\rangle\right) P_{RF}}{cF_\perp}. \tag{33}$$

Furthermore, the second law of thermodynamics can be written for each component ℓ in the form [6]

$$\frac{1}{k_B} d\overset{0}{s}_\ell + \frac{d\overset{0}{P}_{\|,\ell}}{\overset{0}{P}_{\|,\ell}} = d\ln\left[\frac{\overset{0}{T}_\| / \left(m_e c^2\right)}{C_\ell\left(\overset{0}{T},\overset{0}{T}_\|\right)} \exp\left(\frac{m_e\left(\overset{0}{h}_\ell - c^2\right)}{\overset{0}{T}_\|}\right)\right], \tag{34}$$

where k_B is Boltzmann's constant, $\overset{0}{s}_\ell = s_\ell$ is the specific entropy and $\overset{0}{h}_\ell = \overset{0}{H}_\ell / \left(\overset{0}{n}_\ell m_e\right)$ is the specific enthalpy of the component ℓ. The electron stream in ECCD does not perform work and there is no heat addition if the RF power is balanced by power lost through collisions with the background plasma. Therefore, one may take the left-hand side of equation (34) equal to zero putting a constraint on the specific enthalpy of the electron stream (T_0 is a constant):

$$\begin{aligned}(1-F)\overset{0}{h}_0 + F\overset{0}{h}_1 \quad = \quad & c^2 + \frac{\overset{0}{T}_\|}{m_e}(1-F)\ln\left[\left(\frac{T_0}{m_e c^2}\right)^{3/2} \frac{T_0}{\overset{0}{T}_\|} C_0\left(\overset{0}{T},\overset{0}{T}_\|\right)\right] \\ & + \frac{\overset{0}{T}_\|}{m_e} F \ln\left[\left(\frac{T_0}{m_e c^2}\right)^{3/2} \frac{T_0}{\overset{0}{T}_\|} C_1\left(\overset{0}{T},\overset{0}{T}_\|\right)\right].\end{aligned} \tag{35}$$

For a demagnetized stream, i.e. $\overset{0}{T} \to \infty$, this thermodynamic constraint corresponds to an isenthalpic flow. The equations of energy and parallel momentum conservation, and the electrodynamic and thermodynamic constraints give four equations depending on the parameters F, $\left\langle \beta_\| \right\rangle$, $\overset{0}{T}_\|$ and $\overset{0}{T}$ that characterize the distribution function of the energetic current-carrying electrons.

The expression of the parallel force density, $F_\| \sim -neE_\| + n_\| P_{RF}/c$ in Eqs. (14), clearly shows that the RF driven current vanishes when $n_\| \to 0$. For a fully RF driven tokamak plasma the inductive electric field is put equal to zero. In this case the steady-state global figure of merit is defined by

$$\zeta_{RF} = \frac{I_{RF}}{W_{RF}} = \frac{nec\left\langle \beta_{\parallel} \right\rangle A_p}{P_{RF} V_p}, \tag{36}$$

where $I_{RF} = nec\left\langle \beta_{\parallel} \right\rangle \Delta A_p$ is the total RF driven current, $W_{RF} = P_{RF} V_p \Delta A_p / A_p$ is the total input power, $A_p = \pi a^2 \kappa \left(1 - \delta^2/8\right)$ is the area of the poloidal plasma cross-section, $V_p = 2\pi \left(R_0 - a\delta/4\right) A_p$ is the volume of the plasma, and ΔA_p is the effective area of the poloidal plasma cross-section over which the RF power is deposited. The geometrical parameters of the plasma cross-section are: major radius R_0, minor radius a, elongation κ, triangularity δ.

RESULTS AND CONCLUSIONS

Using the macroscopic model a series of equilibrium solutions was determined for the DIII-D tokamak operating conditions. A detailed theoretical scan in $n_{\parallel}$ was made for fixed input power $W_{RF} = 1.5\,\mathrm{MW}$. The following geometrical parameters were considered to characterize the DIII-D tokamak: $R_0 = 1.7\,\mathrm{m}$, $a = 0.6\,\mathrm{m}$, $\kappa = 1.8$, $\delta = 0$ [2, 3]. A typical inductive DIII-D discharge with ECCD produces a RF driven current $I_{RF} = 75\,\mathrm{kA}$, with total plasma current $I_p = 900\,\mathrm{kA}$, central plasma density $n_e = 0.2 \times 10^{20}\,\mathrm{m}^{-3}$, temperature $T_e = 2.7$ keV, and $Z_{eff} = 1.4$. The RF power is produced by four gyrotrons operating at 110 GHz, second-harmonic resonance for a central magnetic induction $B_0 = 2.0\,\mathrm{T}$. In the present model the simplified diffusion coefficient for electron cyclotron fundamental resonance was considered with $\omega = 0.982\Omega_e$. A reference case corresponding to a toroidal angle of incidence $\varphi_T = 20^{\circ}$ ($n_{\parallel} = \sin\varphi_T = 0.342$) and width of the spectrum $\Delta n_{\parallel} = 0.02$ was defined to calibrate the model. The calculation procedure is as follows. The collisional equations of conservation of energy and parallel momentum (4), and the electrodynamic constraint (7) can be used to find the distribution function parameters F, $\left\langle \beta_{\parallel} \right\rangle$, $\overset{0}{T}_{\parallel}$ and $\overset{0}{T}$, and the normalized diffusion coefficient strength $\widehat{D}_0 = D_0 / \left(m_e^2 c^2 \nu_c\right)$, resulting in the experimental figure of merit ζ_{RF} for the given values of the input power W_{RF}, refractive index $n_{\parallel}$ and deposition profile $\Delta A_p / A_p$ (five equations in five unknown quantities). It was found that equilibrium solutions could be determined, corresponding to the input power $W_{RF} = 1.5\,\mathrm{MW}$ and the experimental global figure of merit $\zeta_{RF} = 0.05$ A/W, for values of the relative power deposition area $0.134 < \Delta A_p / A_p < 0.151$ and the normalized diffusion coefficient strength in the range $0.662 < \widehat{D}_0 < 2.24$. Both these quantities can be evaluated, ideally, using a ray-tracing code and the global figure of merit obtained from them. Nevertheless, the values obtained for $\widehat{D}_0$ can be considered as effective values of the diffusion coefficient for the given efficiency, possibly including instabilities (Weibel), trapped particles, and radial transport effects. Note that the obtained range of values of $\Delta A_p / A_p$ closely matches the published measured and simulated results [3]. This method of scanning the quantities in the model is partly justified since all the physics that leads to diffusion is not fully understood.

TABLE 1. Equilibrium parameters for the DIII-D tokamak conditions with $\omega = 0.982\Omega_e$, $\Delta n_{\parallel} = 0.02$, fixed input power $W_{RF} = 1.5\,\mathrm{MW}$, and normalized diffusion coefficient strength $D_0/\left(m_e^2 c^2 \nu_c\right) = 1$.

φ_T	F	$\langle \beta_{\parallel} \rangle$	$\frac{\overset{0}{T}_{\parallel}}{m_e c^2}$	$\frac{\overset{0}{T}}{m_e c^2}$	$\frac{n}{n_e}$	$\frac{\Delta A_p}{A_p}$	$\frac{P_{RF}}{n m_e c^2 \nu_c}$	$\frac{F_{\perp}}{n m_e c \nu_c}$	$\langle \beta_{\perp} \rangle$	$\frac{\overset{0}{T}_{\perp}}{m_e c^2}$
0°	0.628	0	0.252	0.0174	0.0241	0.0447	2.97	16.2	0.183	0.0232
20°	0.562	0.0303	0.100	0.173	0.00901	0.141	2.53	6.93	0.361	0.0918

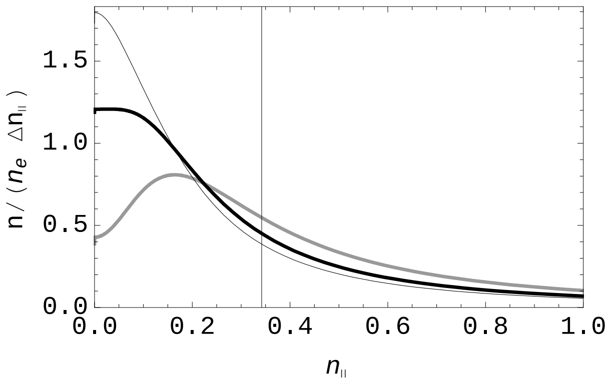

FIGURE 2. Relative density of high-energy electrons in DIII-D. The vertical line indicates the reference value $n_{\parallel} = 0.342$. The thick grey line corresponds to a RF wave frequency $\omega = 0.975\Omega_e$, the thick dark line to $\omega = 0.982\Omega_e$ (reference solution) and the thin dark line to $\omega = 0.985\Omega_e$.

Conversely, one can fix $\widehat{D}_0$ and determine $\Delta A_p/A_p$, which is the procedure adopted in the following. Taking $\widehat{D}_0 = 1$, Table (1) lists the parameters of simulations for steady-state ECCD discharges in the DIII-D tokamak conditions with toroidal launching angles $\varphi_T = 0^\circ$ and 20°. With the equilibrium parameters calculated for the reference launching angle $\varphi_T = 20^\circ$ one evaluates the constant $T_0/(m_e c^2) = 0.310$ which satisfies the thermodynamic constraint (35). Afterwards, the refractive index can be scanned backwards or forwards solving the equations of motion (4), and the electrodynamic and thermodynamic constraints (7) and (35), respectively, maintaining the diffusion coefficient $\widehat{D}_0$ and the input power W_{RF} fixed (again five equations in five unknown quantities). The variation of the refractive index $n_{\parallel}$ must be adiabatic to satisfy the thermodynamic constraint. Note that the calculations involving the equations of motion (4), the electrodynamic constraint (7), and the thermodynamic constraint (35) are independent of the density of resonant electrons. This density appears in the evaluation of the input power W_{RF} and of the total current I_{RF}, in the form of a product of the relative stream density, the width of the spectrum $\Delta n_{\parallel}$ and the effective area of power deposition ΔA_p (the global figure of merit ζ_{RF} is independent of the stream density). Table (1) shows the variation of $\Delta A_p/A_p$ assuming fixed $\Delta n_{\parallel}$, but the same results are obtained assuming fixed $\Delta A_p/A_p$ and varying $\Delta n_{\parallel}$ accordingly. Figure (2) shows the relative density of high-energy electrons in DIII-D, illustrating the rapid decrease in the resonant population for large values of the refractive index $n_{\parallel}$.

Logarithmic plots of the total electron distribution function for the DIII-D conditions are shown in Fig. (3) for $\varphi_T = 0^\circ$ and $\varphi_T = 20^\circ$ at pitch angles of 0°, 90° and 180°. The

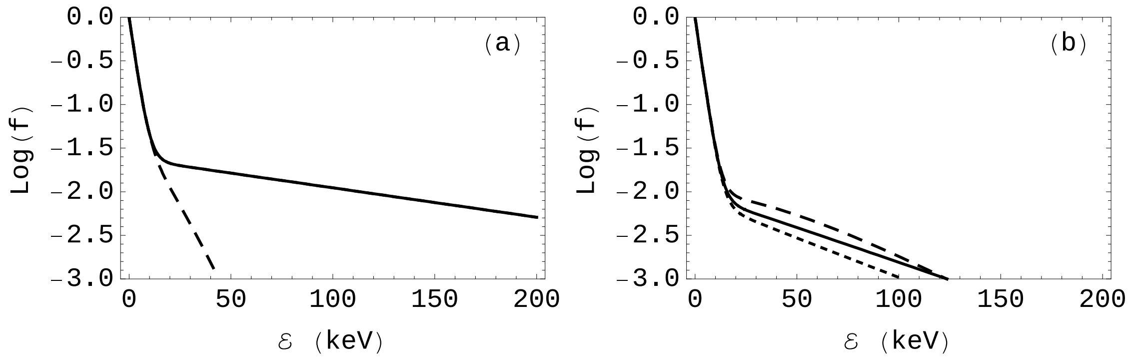

FIGURE 3. Logarithmic plot of the total electron distribution function for (a) $\varphi_T = 0°$ and (b) $\varphi_T = 20°$. The solid, dashed and dotted lines correspond to pitch angles of 0°, 90° and 180°, respectively.

contribution of the high-energy electrons ($\sim$ 128 keV) in the tail of the distribution and along the field lines is clearly seen in the logarithmic plot in Fig. (3a). Obviously, the lines corresponding to pitch angles 0° and 180° are superimposed for $n_{\parallel} = 0$. The energy in the perpendicular direction in momentum space (pitch angle 90°) is much lower, less then 12 keV. Now, for $\varphi_T = 20°$, Fig. (3b) shows that the high-energy electrons ($\sim$ 50 keV) have about the same energy in the parallel and perpendicular directions in momentum space. The small asymmetry between the forward (pitch angle 0°) and backward (pitch angle 180°) directions corresponds to the drift motion with $\langle \beta_{\parallel} \rangle \cong 0.03$. This average stream velocity in the parallel direction increases with $n_{\parallel}$ as expected from equation (14) for the parallel force.

A few results of the refractive index scan performed for the DIII-D conditions is shown in Fig. (4) with $\Delta n_{\parallel} = 0.02$, fixed input power $W_{RF} = 1.5\,\mathrm{MW}$, and normalized diffusion coefficient strength $D_0/\left(m_e^2 c^2 \nu_c\right) = 1$. The grey circles correspond to $\omega = 0.975\Omega_e$, the black circles to $\omega = 0.982\Omega_e$ (reference solution), and the dots to $\omega = 0.985\Omega_e$. The vertical line indicates the reference value $n_{\parallel} = 0.342$. Equilibrium can not be achieved in the present model for values of the refractive index larger than shown in the graphics. Presumably, runaway electrons are excited for larger values of $n_{\parallel}$, invalidating the fluid model. The global figure of merit shown in Fig. (4a) closely follows the increase in the average parallel velocity of the streaming electrons. The perpendicular temperature shown in Fig. (4b) increases and attains the maximum level approximately given by Eq. (26) for $\overset{0}{T} \to \infty$, implying demagnetization of the high-energy stream. This demagnetization process is accompanied by a cooling of the electron stream in the parallel direction. The increase in the perpendicular temperature, from the 12 keV to the 60 keV level ($m_e c^2 \cong 511$ keV) as the toroidal launching angle increases from 0° to 25°, reproduces the results obtained with a hard X-ray (HXR) pinhole camera in the toroidal injection angle sweeping experiment performed in TCV [4]. Although the present results refer to the DIII-D tokamak conditions, very similar results are obtained for TCV. The main differences are the much larger relative stream density and significantly larger effective area of power deposition in the TCV case, taking into account the large power input (same level as in DIII-D) over a much smaller plasma volume.

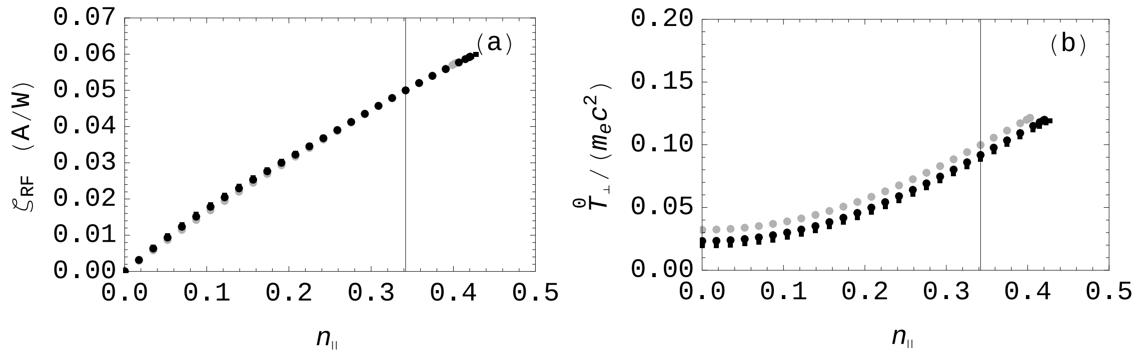

FIGURE 4. Global figure of merit (a) and normalized perpendicular temperature of the electron stream (b) as functions of the parallel refractive index (note that $m_e c^2 \cong 511$ keV).

In conclusion, a macroscopic model based on a suitable distribution function of the current-carrying electrons has been developed which reproduces the main features of ECCD experiments. By choosing an effective value of the diffusion coefficient strength, the experimental value of the global figure of merit is obtained at input power levels and power deposition areas equivalent to the measured ones. A theoretical sweep of the toroidal angle of injection reproduces both the variation of the global figure of merit and the signature of the high-energy electrons in the perpendicular plane, as detected by HXR measurements. In this way, the proposed form of the distribution function may become an useful tool for fitting ECCD experimental results. It may also become useful for studying the time evolution of ECCD and the possible occurrence of instabilities. The model can be improved in several ways, mostly by including trapped particle effects.

ACKNOWLEDGMENTS

This work was partially supported by the International Atomic Energy Agency under the Coordinated Research Project on Joint Research Using Small Tokamaks – IAEA Contract No. BRA/12932.

REFERENCES

1. O. Sauter *et al.*, "Steady-state fully noninductive current driven by electron cyclotron waves in a magnetically confined plasma", *Phys. Rev. Lett.* **84** 3322-3325 (2000).
2. R.W. Harvey *et al.*, "Radial transport and electron-cyclotron-current drive in the TCV and DIII-D tokamaks", *Phys. Rev. Lett.* **88** 205001(4) (2002).
3. C.C. Petty *et al.*, "Detailed measurements of the electron cyclotron current drive efficiency on DIII-D", *Nucl. Fusion* **42** 1366-1375 (2002).
4. S. Coda *et al.*, "Electron cyclotron current drive and suprathermal electron dynamics in the TCV tokamak", *Nucl. Fusion* **43** 1361-1370 (2003)
5. K. Hizanidis, and A. Bers, "Steady-state rf-current drive theory based upon the relativistic Fokker-Planck equation with quasilinear diffusion", *Phys. Fluids*, **27** 2669-2675 (1984).
6. G.O. Ludwig, "Relativistic distribution functions, fluid equations and equations of state for magnetized electron streams", *Plasma Phys. Control. Fusion*, **49** 1521-1549 (2007).